IEEE Life Sciences Letters

Received 9 November 2015; revised 22 July 2016; accepted 1 October 2016. Date of publication 26 December 2016; date of current version 27 January 2017.

Digital Object Identifier 10.1109/LLS.2016.2644646

A Temporal Logic Inference Approach for Model Discrimination

ZHE XU[1], MARC BIRTWISTLE[2], CALIN BELTA[3], AND AGUNG JULIUS[1]

[1]Electrical, Computer, and Systems Engineering Department, Rensselaer Polytechnic Institute, Troy, NY 12180 USA

[2]Icahn School of Medicine at Mount Sinai, New York, NY 10029 USA

[3]Boston University, Boston, MA 02215 USA

CORRESPONDING AUTHOR: Z. XU (xuz8@rpi.edu)

This work was supported by the National Science Foundation under Grant CNS-0953976 and Grant EF-1137906.

ABSTRACT We propose a method for discriminating among competing models for biological systems. Our approach is based on learning temporal logic formulas from data obtained by simulating the models. We apply this method to find dynamic features of epidermal growth factor induced extracellular signal-regulated kinase (ERK) activation that are strictly unique to positive versus negative feedback models. We first search for a temporal logic formula from a training set that can eliminate ERK dynamics observed with both models and then identify the ERK dynamics that are unique to each model. The obtained formulas are tested with a validation sample set and the decision rates and classification rates are estimated using the Chernoff bound. The results can be used in guiding and optimizing the design of experiments for model discrimination.

INDEX TERMS Extracellular signal-regulated kinase (ERK), model discrimination, temporal logic.

I. INTRODUCTION

MATHEMATICAL models can be used to generate hypotheses that can guide experiments of biological systems. How to select better models and check which model is more representative of the real biological systems has always been a challenge. This subject in modeling is often called model discrimination [1]–[7].

There is rich literature on designing methods for model discrimination. Most of the methods are based on statistical analysis such as maximal likelihood and the main goal is to design input such that the outputs of different models can be more different [8]. As the models from systems biology are usually nonlinear, for example, arising from mass action kinetics or enzyme kinetics, usually linearization is an essential part in the input design for model discrimination [9], [10].

In recent years, temporal logics have been increasingly used in expressing more complicated and precise statements that often occur in real systems [11]–[13]. It is a set of rules for representing and analyzing the temporal behavior of physical and biological systems. The temporal logic that we use is called signal temporal logic (STL) [14]. STL formulas are evaluated on time trajectories. For example, the time trajectory $x(t) = \sin(t)$ satisfies the formula $\square_{(0,\pi)}(x > 0)$, which reads as "During the time interval of $(0, \pi)$, $x(t)$ is always greater than 0." STL can be used to express quantitative high-level features of a group of simulated time trajectories from various models. The comparison of these features with those of the experimentally generated trajectories allows us to determine which model fits the system's behavior better. Kong *et al.* [15] have designed an inference algorithm that can automatically derive temporal logic formulas that can classify trajectories in different sets directly from data. We apply their algorithm in model discrimination by discriminating among trajectories generated by different competing mathematical models. Under certain circumstances, the algorithm can lead to misclassification (which means that certain trajectories are wrongly classified by the formula), for example, if some trajectories generated by one model are the same as or very similar to some trajectories generated by the other model. In this letter, we present a new method that can largely reduce the misclassification rate in discriminating between different trajectories generated by different mathematic models. We first search for a temporal logic formula that can eliminate the trajectories that are the same or very similar for both models. Then we classify only the remaining trajectories for both models with another temporal logic formula.

This letter is structured as follows. Section II shows the problem formulation. Section III shows the new approach. Section IV describes the implementation on the extracellular signal-regulated kinase (ERK) pathway. Finally, some conclusions are presented in Section V.

II. PROBLEM FORMULATION

Assume we have two mathematical models, Model 1 and Model 2, that we want to discriminate. In this letter, both models are assumed to be stochastic. For Models 1 and 2, we

have probability spaces $(\Omega_i, \mathcal{F}_i, P_i)_{i=1,2}$, respectively [16]. Each simulation of the models is considered as a map from Ω_i to the space of trajectories. We assume that these spaces are not explicitly specified. Rather, we assume that we can generate sample trajectories that are mapped from independent samples from these probability spaces.

The problem that we consider in this letter is to find an STL formula ϕ that separates trajectories from Models 1 and 2. That is, ϕ is satisfied by (trajectories from) Model 1 with high probability and violated by (trajectories from) Model 2 with high probability. Here, we assume that the subsets of Ω_i corresponding to the satisfaction/violation of the STL formula that we consider are measurable in $\mathcal{F}_i$.

We seek to solve this problem by working with sample trajectories generated from both models. That is, we seek to solve the following problem.

Problem 1: We denote Set1_t *and* Set2_t *as two training sets of trajectories generated by Model* 1 *and Model* 2 *(generated stochastically by sampling initial conditions or modeling parameters, etc.). Find a temporal logic formula to discriminate trajectories in* Set1_t *and* Set2_t.

We denote the L_∞ norm of a trajectory s as $\|s\|_\infty = \sup_{0\le t\le T} \|s(t)\|$. Note that some trajectories in Set1_t may be the same as or very similar to some trajectories in Set2_t, i.e., there exist subsets $\text{Sub1}_t \subset \text{Set1}_t$ and $\text{Sub2}_t \subset \text{Set2}_t$ defined as follows:

$$\begin{aligned}\text{Sub1}_t &\triangleq \{s_1 \in \text{Set1}_t \mid \exists s_2 \in \text{Set2}_t, \|s_1 - s_2\|_\infty \le \epsilon\}\\ \text{Sub2}_t &\triangleq \{s_2 \in \text{Set2}_t \mid \exists s_1 \in \text{Set1}_t, \|s_1 - s_2\|_\infty \le \epsilon\} \quad (1)\end{aligned}$$

where ϵ is a small positive number.

III. SOLUTION

A. TEMPORAL LOGIC INFERENCE

Using the inference algorithm in [15], we search for the temporal logic formula ϕ that is best satisfied by the trajectories in Set1_t and violated by the trajectories in Set2_t. The temporal logic formula ϕ has the form $\phi = (A \Rightarrow B)$, with A being the cause and B being the effect formula.

If some trajectories in Set1_t are the same as or very similar to some trajectories in Set2_t (i.e., Sub1_t and Sub2_t exist), then the algorithm would give us a temporal logic formula ϕ with positive misclassification rate. There are some "mirror" trajectories in the other set that are not misclassified, but are the same as or very similar to the misclassified trajectories. It can be seen from Fig. 1 that the sets Sub1_t and Sub2_t are the reason for the misclassified trajectories.

In order to better discriminate the two models, we propose a modified method that can largely reduce the misclassification rate. We intend to derive the temporal logic formula ϕ' of the form $\phi' = (A' \overset{\Delta}{\Rightarrow} B')$, where the newly defined logical symbol " $\overset{\Delta}{\Rightarrow}$ " is different from the "implication" symbol " $\Rightarrow$ " and the new truth table is shown in Table 1. Unlike formula A, formula A' serves an entirely different function: it is designed as a criterion to determine the decidability of the discrimination. We denote $\text{Sub1}'_t \triangleq \text{Set1}_t \setminus \text{Sub1}_t$ and $\text{Sub2}'_t \triangleq \text{Set2}_t \setminus \text{Sub2}_t$ as the subsets of trajectories in Set1_t and Set2_t that are not similar and should be separated completely (as shown in Fig. 1).

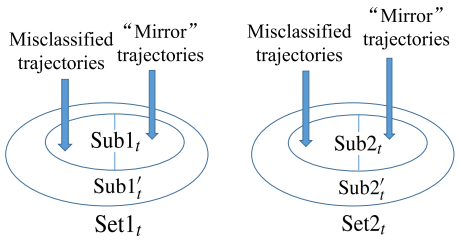

FIGURE 1. Diagram of the different subsets of the training set.

TABLE 1. Truth Table of $A' \overset{\Delta}{\Rightarrow} B'$

A'	B'	$A' \overset{\Delta}{\Rightarrow} B'$
T	T	T
T	F	F
F	T	Undecidable
F	F	Undecidable

We thus can run the algorithm in [15] to search for temporal logic formula A' that is best satisfied by trajectories in $\text{Sub1}'_t \cup \text{Sub2}'_t$ and violated by trajectories in $\text{Sub1}_t \cup \text{Sub2}_t$.

After that, we run the algorithm to search for temporal logic B' that is best satisfied by trajectories in $\text{Sub1}'_t$ and violated by trajectories in $\text{Sub2}'_t$. In this way, the two sets $\text{Sub1}'_t$ and $\text{Sub2}'_t$ can be completely separated based on property B'. Specifically, $\text{Sub1}'_t$ (which is generated by Model 1) satisfies B', and $\text{Sub2}'_t$ (which is generated by Model 2) does not.

B. TEMPORAL LOGIC TESTING

We check the validity of the formula with the validation sample set (the validation sample set is independent of the training sample set). We denote the trajectories generated stochastically by Model 1 and Model 2 in the validation sample set as Set1_v and Set2_v. Similarly, we define Sub1_v and Sub2_v as follows:

$$\begin{aligned}\text{Sub1}_v &\triangleq \{s_1 \in \text{Set1}_v \mid \exists s_2 \in \text{Set2}_v, \|s_1 - s_2\|_\infty \le \epsilon\}\\ \text{Sub2}_v &\triangleq \{s_2 \in \text{Set2}_v \mid \exists s_1 \in \text{Set1}_v, \|s_1 - s_2\|_\infty \le \epsilon\}. \quad (2)\end{aligned}$$

We denote $\text{Sub1}'_v \triangleq \text{Set1}_v \setminus \text{Sub1}_v$ and $\text{Sub2}'_v \triangleq \text{Set2}_v \setminus \text{Sub2}_v$. We calculate the decision rate and classification rates using the following formula:

$$\begin{aligned}\hat{P}_{d1} &= n(\text{Sub1}'_v)/n(\text{Set1}_v)\\ \hat{P}_{d2} &= n(\text{Sub2}'_v)/n(\text{Set2}_v)\\ \hat{P}_{c1} &= n(\text{Sub1}''_v)/n(\text{Sub1}'_v)\\ \hat{P}_{c2} &= n(\text{Sub2}''_v)/n(\text{Sub2}'_v) \quad (3)\end{aligned}$$

where $\hat{P}_{d1}$ and $\hat{P}_{d2}$ are the decision rates for Set1_v and Set2_v, respectively (i.e., the percentage of trajectories that can be definitely classified by the formula); $\hat{P}_{c1}$ and $\hat{P}_{c2}$ are the classification rates for Set1_v and Set2_v, respectively (i.e., the percentage of trajectories that is rightly classified by the formula); $n(\text{Set1}_v)$ and $n(\text{Set2}_v)$ denote the number

IEEE Life Sciences Letters

of trajectories in Set1_v and Set2_v, respectively; $n(\text{Sub1}'_v)$ and $n(\text{Sub2}'_v)$ denote the number of trajectories in sets $\text{Sub1}'_v$ and $\text{Sub2}'_v$, respectively (i.e., satisfying A'); and $n(\text{Sub1}''_v)$ denotes the number of trajectories in set $\text{Sub1}'_v$ that satisfies B' and $n(\text{Sub2}''_v)$ denotes the number of trajectories in set $\text{Sub2}'_v$ that violates B'.

We use the following Chernoff bounds [16] to estimate the expected probabilities for the decision rates and classification rates for each model:

$$P\{\hat{p} \geq p + \alpha\} \leq e^{-N\alpha^2/3}$$
$$P\{\hat{p} \leq p - \alpha\} \leq e^{-N\alpha^2/2} \tag{4}$$

where $\hat{p}$ and p are the calculated probability in the validation sample set and the actual probability, respectively. The precision of such an assessment depends on the total number of trajectories N, so a larger N would give a tighter bound for the estimate.

IV. IMPLEMENTATION

In this section, we apply the proposed approach to discriminate two models in systems biology. We simulate the ERK responses to epidermal growth factor (EGF) treatment. By changing the feedback strength parameter (Fa), we create two different continuous-time ordinary differential equation models with nine variables: Model 1 with positive feedback and Model 2 with negative feedback. Positive feedback loops enforce all-or-nothing and switch-like sharp dose responses typically corresponding to cell fates, whereas negative feedback has typically smooth dose responses associated with analog control biologically. Thus, distinguishing the feedback mode has mechanistic interpretations for the pathway biological function. The parameters of the models are taken from a previous model of ERK/MAPK signaling in [17]. These in turn were predominantly taken from biochemical enzyme kinetic experimental studies. Specifically, we used a flow cytometry-based phosphorylation assay to determine the kinetics and dose response of ERK activation by the EGF in HEK293 cells. From each model, for certain EGF doses, we simulate many time trajectories of activated (dually phosphorylated) ppERK levels of individual "cells" (Fig. 2) by sampling total protein levels from a gamma distribution for initial conditions and then simulating with deterministic ordinary differential equation (ODE) solvers according to the rate equations.

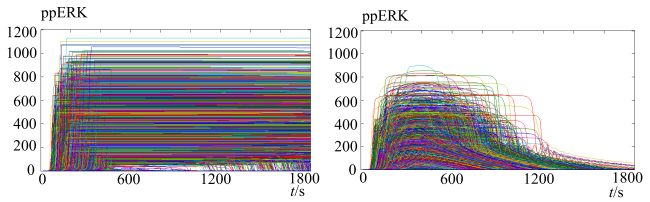

FIGURE 2. Trajectories generated from Model 1 (left) and Model 2 (right) with an EGF dose of 0.1 nM using 20 000 trajectories generated from Model 1 and 20 000 trajectories from Model 2.

We first use the algorithm in [15] to search for the temporal logic formula that is best satisfied by trajectories in Model 1 and violated by trajectories in Model 2. We generate 50 trajectories from each model as the training sample set for the STL inference. We use x to denote the ppERK level and the following formula can be obtained with 20% misclassification rate (which means that 20% of the trajectories of the two models are wrongly classified by the formula):

$$\begin{aligned}\phi \;&=\; (\text{dose} = 0.1) \wedge \Diamond_{[10,110.029]}(x < 1.0013) \\ &\Rightarrow \Box_{[1700,1800]}(x > 52.774).\end{aligned} \tag{5}$$

The formula reads as "If dose = 0.1 nM and the ppERK level is lower than 1.0013 nM for at least one point in the time period [10,110.029]s, then the ppERK level is always higher than 52.774 nM for the time period [1700,1800]s."

As can be seen in Fig. 3, compared with Model 2, the trajectories generated by Model 1 have a general trend of maintaining higher ppERK levels after EGF stimulation. However, in both Models 1 and 2, there is a fraction of trajectories with ppERK levels close to 0. This approximately "overlapping" (we use double quote as they can be very similar and not actually overlapped) part is the reason for the 20% misclassification rate. Specifically, we find that all misclassified trajectories belong to Sub1_t and their "mirror" trajectories belong to Sub2_t. We first find the trajectories in Sub1_t and Sub2_t. Sub1_t can be obtained by seeking out the trajectories in Set1_t that have at least one trajectory in Set2_t that is the same or very similar using the L_∞ norm (we set ϵ to be 1), and their "mirror" trajectories in Set2_t are the trajectories in Sub2_t. With the modified method, we are able to calculate the following formulas with 0% misclassification rate. There are 30 trajectories in $\text{Sub1}'_t$, 20 trajectories in Sub1_t, 30 trajectories in $\text{Sub2}'_t$, and 20 trajectories in Sub2_t. The calculation takes about 56 s on a laptop PC

$$\begin{aligned}\phi' \;&=\; (A' \overset{\Delta}{\Rightarrow} B') \\ A' \;&=\; (\text{dose} = 0.1) \wedge \Box_{[282.9834,505.1982]}(x > 3.5114) \\ B' \;&=\; \Diamond_{[900,1800]}(x > 118.6944).\end{aligned} \tag{6}$$

The formula A' reads as "the dose = 0.1 nM and the ppERK level is always higher than 3.5114 nM for the time period [282.9834,505.1982]s." The formula B' reads as "the ppERK level is higher than 118.6944 nM for at least one point in the time period [900,1800]s."

Using the same approach, we can infer the following formulas with different EGF doses:

$$\begin{aligned}\phi'_2 \;&=\; (A'_2 \overset{\Delta}{\Rightarrow} B'_2) \\ A'_2 \;&=\; (\text{dose} = 0.5) \wedge \Diamond_{[10,642.2807]}(x > 31.9832) \\ B'_2 \;&=\; \Diamond_{[1017.9337,1800]}(x > 181.7557)\end{aligned} \tag{7}$$

$$\begin{aligned}\phi'_3 \;&=\; (A'_3 \overset{\Delta}{\Rightarrow} B'_3) \\ A'_3 \;&=\; (\text{dose} = 1) \wedge \Diamond_{[10,712.8703]}(x > 113.5725) \\ B'_3 \;&=\; \Box_{[900,1216.9086]}(x > 173.4933)\end{aligned} \tag{8}$$

$$\phi'_4 = (A'_4 \overset{\Delta}{\Rightarrow} B'_4)$$

$$A'_4 = (\text{dose} = 5) \wedge \Diamond_{[10,617.2902]}(x > 0.0139)$$
$$B'_4 = \Box_{[1199.3912,1493.8374]}(x > 130.494) \quad (9)$$
$$\phi'_5 = (A'_5 \overset{\Delta}{\Rightarrow} B'_5)$$
$$A'_5 = (\text{dose} = 10) \wedge \Diamond_{[10,900]}(x > 0.0509)$$
$$B'_5 = \Box_{[1204.276,1605.0666]}(x > 165.494). \quad (10)$$

We further test the validity of this formula in the validation sample set of 20 000 trajectories generated by the mathematical models, and the decision rates and classification rates for each model calculated by (3) are shown in Table 2.

TABLE 2. Decision Rates and Classification Rates in the Validation Sample

dose(nM)	$\hat{P}_{d1}$	$\hat{P}_{d2}$	$\hat{P}_{c1}$	$\hat{P}_{c2}$
0.01	0%	0%	0%	0%
0.1	52.73%	51.48%	96.95%	96.84%
0.5	90.58%	87.37%	88.56%	94.87%
1	95.18%	90.49%	91.69%	96.82%
5	99.93%	99.93%	93.07%	94.18%
10	99.98%	99.98%	89.51%	90.32%

TABLE 3. Estimated Decision Rates and Classification Rates

dose(nM)	P_{d1}	P_{d2}	P_{c1}	P_{c2}
0.01	0%	0%	0%	0%
0.1	$\geq$ 50.10%	$\geq$ 48.85%	$\geq$ 93.33%	$\geq$ 93.18%
0.5	$\geq$ 87.95%	$\geq$ 84.74%	$\geq$ 85.80%	$\geq$ 92.06%
1	$\geq$ 92.55%	$\geq$ 87.86%	$\geq$ 89.00%	$\geq$ 94.06%
5	$\geq$ 97.30%	$\geq$ 97.30%	$\geq$ 90.44%	$\geq$ 91.55%
10	$\geq$ 97.35%	$\geq$ 97.35%	$\geq$ 86.88%	$\geq$ 87.69%

Using the Chernoff bound in (4), we can calculate for 99% confidence level the estimated decision rates and classification rates for each model, as shown in Table 3. It can be seen that for an EGF dose of 5 nM, the overall performance is better with regard to the estimated decision rates and classification rates for each model compared with that for the other doses. Based on this, we can use ϕ'_4 to design the following experiment. First, use the EGF dose of 5 nM and observe whether the ppERK level is higher than 0.0139 nM for at least one point in the time period [10, 617.2902]s; if the answer is no, then it cannot be decided which model it is; if the answer is yes, then observe whether the ppERK level is always higher than 130.494 nM for the time period [1199.3912, 1493.8374]s. If the answer is yes, then accept Model 1; otherwise, accept Model 2. Of course, more complex inference into subsequent experiments and model discrimination is possible with the described approach.

V. CONCLUSION

In this letter, we use an inference algorithm to extract the temporal logic properties of ERK responses to EGF stimulation and propose a new method for model discrimination by searching for temporal logic formulas from simulation trajectories. We define the decision rates and classification rates of temporal logic formulas in model discrimination. We test the obtained temporal logic formulas with a validation sample set and provide guidelines for experiment design based on the decision rates and classification rates estimated using the Chernoff bound. The obtained formula shows the temporal logic properties of the various cell responses, which is useful in designing experiments for model discrimination.

REFERENCES

[1] R. M. Engeman, G. D. Swanson, and R. H. Jones, "Input design for model discrimination: Application to respiratory control during exercise," *IEEE Trans. Biomed. Eng.*, vol. BME-26, no. 10, pp. 579–585, Oct. 1979.

[2] A. Hamadeh, B. Ingalls, and E. Sontag, "Fold-change detection as a chemotaxis model discrimination tool," in *Proc. IEEE 51st Annu. Conf. Decision Control (CDC)*, Dec. 2012, pp. 5523–5527.

[3] P. Rodríguez, "Noise model discrimination for digital images based on variance-stabilizing transforms and on local statistics: Preliminary results," in *Proc. 45th Asilomar Conf. Signals, Syst. Comput. (ASILOMAR)*, Nov. 2011, pp. 728–732.

[4] D. R. Cavagnaro, J. I. Myung, M. A. Pitt, and J. V. Kujala, "Adaptive design optimization: A mutual information-based approach to model discrimination in cognitive science," *Neural Comput.*, vol. 22, no. 4, pp. 887–905, 2010.

[5] L. Blackmore and B. Williams, "Finite horizon control design for optimal model discrimination," in *Proc. 44th IEEE Conf. Decision Control, Eur. Control Conf. (CDC-ECC)*, Dec. 2005, pp. 3795–3802.

[6] K. W. Hipel, "Geophysical model discrimination using the Akaike information criterion," *IEEE Trans. Autom. Control*, vol. 26, no. 2, pp. 358–378, Apr. 1981.

[7] K. Uosaki, I. Tanaka, and H. Sugiyama, "Optimal input design for autoregressive model discrimination with constrained output variance," *IEEE Trans. Autom. Control*, vol. 29, no. 4, pp. 348–350, Apr. 1984.

[8] S. Cheong and I. R. Manchester. (Oct. 2013). "Input design for model discrimination and fault detection via convex relaxation." [Online]. Available: https://arxiv.org/abs/1310.7262

[9] D. Georgiev, M. Fazel, and E. Klavins, "Model discrimination of chemical reaction networks by linearization," in *Proc. Amer. Control Conf. (ACC)*, Jun. 2010, pp. 5916–5922.

[10] D. Georgiev and E. Klavins, "Model discrimination of polynomial systems via stochastic inputs," in *Proc. 47th IEEE Conf. Decision Control*, Dec. 2008, pp. 3323–3329.

[11] C. Baier and J.-P. Katoen, *Principles of Model Checking (Representation and Mind Series)*. Cambridge, MA, USA: MIT Press, 2008.

[12] Z. Xu, C. Belta, and A. Julius, "Temporal logic inference with prior information: An application to robot arm movements," in *Proc. IFAC Conf. Anal. Design Hybrid Syst. (ADHS)*, 2015, vol. 48. no. 27, pp. 141–146.

[13] Z. Xu and A. A. Julius, "Census signal temporal logic inference for multiagent group behavior analysis," *IEEE Trans. Autom. Sci. Eng.*, to be published. [Online]. Available: http://ieeexplore.ieee.org/document/7587357/

[14] A. Donzé and O. Maler, "Robust satisfaction of temporal logic over real-valued signals," in *Proc. 8th Int. Conf. (FORMATS)*, Berlin, Germany, 2010, pp. 92–106. [Online]. Available: http://dl.acm.org/citation.cfm?id=1885174.1885183

[15] Z. Kong, A. Jones, A. M. Ayala, E. A. Gol, and C. Belta, "Temporal logic inference for classification and prediction from data," in *Proc. 17th Int. Conf. Hybrid Syst., Comput. Control (HSCC)*, New York, NY, USA, 2014, pp. 273–282.

[16] M. Mitzenmacher and E. Upfal, *Probability and Computing: Randomized Algorithms and Probabilistic Analysis*. Cambridge, U.K.: Cambridge Univ. Press, 2005. [Online]. Available: https://books.google.com/books?id=0bAYl6d7hvkC

[17] M. Birtwistle *et al.*, "Emergence of bimodal cell population responses from the interplay between analog single-cell signaling and protein expression noise," *BMC Syst. Biol.*, vol. 6, no. 1, p. 109, 2012.